https://doi.org/10.2352/ISSN.2169-2629.2018.26.140

White Balance under White-light LED Illumination

Siyuan Chen, Minchen Wei*; Department of Building Services Engineering, The Hong Kong Polytechnic University; Hong Kong.
****Minchen.wei@polyu.edu.hk***

Abstract

Conventional light sources (e.g., fluorescent) contain UV/violet radiations that can excite the fluorescent whitening agents (FWAs) in man-made and natural white objects to enhance whiteness appearance and create different degrees of white. Typical white-light LED sources, however, contain little UV/violet radiation to increase its luminous efficacy. In this study, we investigated how the failure of white-light LEDs to excite FWAs affect the image color appearance with different white balance algorithms. A same setup, including a Macbeth ColorChecker and three whiteness standards with different amount of FWAs, were illuminated by two 6500 K illuminants with different levels of UV/violet radiation. The captured RAW images were white balanced using 10 algorithms. It was found the failure of FWA excitation produced noticeable color differences, with an average ΔE from 2.9 to 8.1 in the CIELAB color space. The algorithms based on the Gray World assumption were generally less sensitive to the FWA excitation, in comparison to those based on the Retinex theory.

Introduction

Whiteness, an important colorimetric characteristic for surface colors, is commonly associated with product quality, which has attracted the attention of researchers and manufacturers. Fluorescent whitening agents (FWAs), a material that absorbs ultraviolet (UV)/violet radiation from illumination and re-emits blue radiation, can enhance the whiteness appearance of surface colors and are widely used in man-made objects. Conventional light sources always contain some UV/violet radiation to excite the FWAs in surface colors [1]. In contrast, manufacturers seldom include UV/violet radiation in white-light LED sources, as it depletes luminous efficacy. It has been found that the failure of typical white-light LEDs to excite FWAs can produce a noticeable decrease of whiteness appearance to human perception [2-4]. Little attention has been paid to how imaging systems respond to such a failure, though white appearance is critical in image process and image quality [5].

White balance, a function incorporated in imaging systems to simulate the mechanism of chromatic adaptation in human color vision, adjusts colors in an image to eliminate the color cast of the illumination and reproduce the color appearance perceived by humans to some extent. Various white balance algorithms have been developed, most of which were based on either the Gray World assumption [6] or the Retinex theory [7] (a.k.a., Perfect Reflector [8] or White Patch assumption [9]). The former assumes that a captured image is achromatic on average, with the average RGB values being equal. Such an assumption is more likely to be held when a scene does not have a dominant color [10]; the latter assumes that the color of the pixel(s) with the highest RGB values of an image is the color of the illuminant.

The GW algorithm and the maxRGB algorithms, the two simplest algorithms based on the Gray World assumption and the Retinex theory respectively, can be described using Eq. (1), with a Minokowski norm (i.e., p) of 1 and $+\infty$ respectively [11]. The calculated Minokowski means t_c (C = R, G, and B), which are the average and the highest RGB values of an image respectively, are then used to calculate the gain factors for R and B values (i.e., *corrR* and *corrB*) as Eq. (2) and to derive the balanced R and B values (i.e., *R*' and *B*') using Eq. (3) (Note: the G values are typically kept unchanged). Instead of using extreme values, the Shades-of-Gray (SoG) algorithm [11] was proposed to use a p value between 1 and $+\infty$, with a p between 2 and 29 being suggested to have a better performance.

$$t_C = \left(\frac{\sum I_C(x)^p}{N}\right)^{\frac{1}{p}} \tag{1}$$

$$corrR = \frac{t_G}{t_R},\ corrB = \frac{t_G}{t_B} \tag{2}$$

$$R' = corrR \times R, G' = G, B' = corrB \times B \tag{3}$$

where C denotes R, G, or B; $I(x)$ is the R, G, or B value of each pixel; N is the number of pixels in an image; and p is the Minkowski norm.

Various modifications on the GW and the maxRGB algorithms have been proposed to improve their performance and robustness. The Modified Gray World (MGW) algorithm [12] calculates the gain factors by allowing a small variation between the average RGB values of an image. The Standard Deviation Weighted Gray World (SDWGW) algorithm [10] divides an image into blocks and puts higher weights to the blocks with a larger variation of the RGB values when calculating the standard deviation weighted average (SDWA). The Itr+GWA algorithm [13] transforms the *RGB* values of each pixel to *YUV* values and detects the "gray pixels". The gain factors are then iteratively adjusted until the average U and V values of the gray pixels are close to zero (i.e., < 0.001). The Auto Level algorithm [14] extends the concept of the Retinex theory by scaling the RGB values of each pixel linearly in relative to the maximum and minimum RGB values of an image. The maximum and minimum 0.5% of the RGB values are then discarded. Efforts were also made to combine the GW and the maxRGB algorithms. The GWR algorithm [15] transforms the R and B values using quadratic functions, so that both the average and highest RGB values are equal in a balanced image.

It can be observed that the color of each pixel affects the color appearance of a balanced image via white balance algorithms. For the algorithms relying on the brightest or the neutral pixel(s), the impact of the white surfaces is particularly important. This study aimed to quantify the change of image color appearance using various white balance algorithms caused by the failure of white-light LEDs to excite FWAs.

Method

A viewing booth and a spectrally tunable LED device (manufactured by THOUSLITE, Changzhou, China) were used in this study. The dimensions of the viewing booth were 50 cm (width) × 50 cm (depth) × 60 cm (height) and the interiors were painted with Munsell N7 neutral gray paint. The spectrally tunable LED device, which had 14 channels with peak wavelengths covering a range from 350 to 680 nm, was placed above the booth to provide a uniform illumination, as verified in a previous study [16]. A Macbeth ColorChecker and three calibrated diffuse whiteness standards containing different amount of FWAs were placed on a 45° viewing table in the booth, as shown in Fig 1. The three whiteness standards, labelled as $W_{84.4}$, $W_{121.6}$, and $W_{138.9}$, had a CIE whiteness value of 84.4, 121.6, and 138.9, with a higher value indicating a greater amount of FWAs. These three standards covered the range of whiteness appearance that are commonly around us.

Figure 1. A photograph of the experiment setup, which was taken under the illuminant with normal UV/violet radiation.

The SPDs of the two 6500K illuminants were carefully designed to produce two levels of UV/violet radiations (i.e., low and normal). The violet emission levels, the percentage of the radiant power below 430 nm to the overall radiant power [1], of the two illuminants were 2.7% and 16.1%. The former was designed to mimic typical blue-pumped white LEDs, with the average violet emission level of 3.6% being calculated from a large dataset [17]; the latter was designed to mimic CIE standard D65 that has a violet emission level of 17.4%. Table I summarizes the colorimetric characteristics of the two illuminants. The illuminants were calibrated to provide an illuminance of 1000 ± 10 lx at the center of the viewing table using a calibrated Minolta T-10 illuminance meter; the SPDs, as shown in Fig. 2, were measured using a calibrated JETI 1411UV specbo spectroradiometer with a white standard.

A Canon EOS 80D camera was used to capture two images, with one under the low UV/violet illuminant and the other under the normal UV/violet illuminant. The RAW images were stored in the CR2 format with a resolution of 6000 × 4000. The workflow, as shown in Fig. 3, was followed to process the two RAW images using different white balance algorithms. The average (L^*,a^*,b^*) of the 100 × 100 pixels at the center of each color patch and whiteness standard was used in the following analyses.

Table I Colorimetric characteristics of the two illuminants

UV/violet level	CCT (K)	D_{uv}	x	y	CRI-R_a	M_v	M_u
Low	6588	+0.008	0.310	0.335	94	1.49	6.07
Normal	6461	+0.004	0.313	0.330	98	0.62	1.50

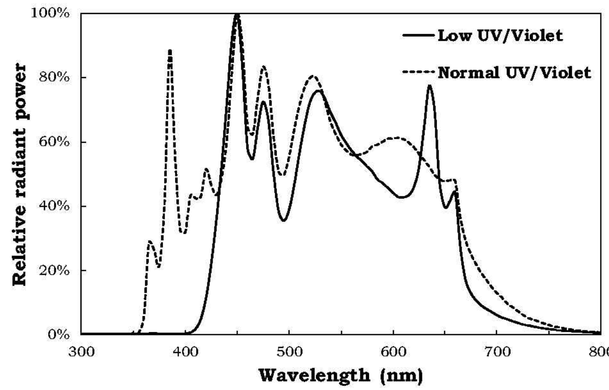

Figure 2. The relative SPDs of the two illuminants.

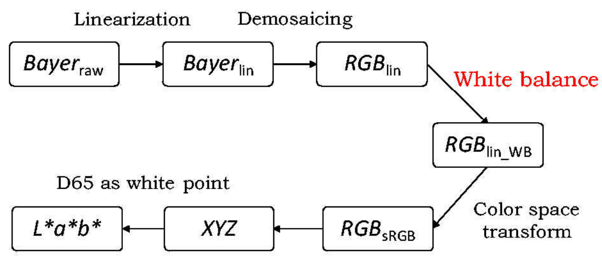

Figure 3 The workflow for calculating the chromaticity coordinates from the raw images

Results

Figure 4 shows the average color difference (i.e., ΔE) of the 24 Macbeth Color patches and the three whiteness standards between the two balanced images in CIELAB color space using each algorithm. It can be observed that the amount of UV/violet radiations contained in the illuminants always produced noticeable color differences, regardless of which algorithm was used. Specifically, the images using the algorithms based on the Gray World assumption (i.e., GW, MGW, SDWGW, and Itr+GWA) had smaller color differences than those using the algorithms based on the Retinex theory (i.e., maxRGB and Auto Level). Furthermore, the color differences for those using the SoG algorithms were between those using the Gray World assumption and the Retinex theory, with larger Minkowski norm (i.e., p) values producing larger color differences and making the algorithm more similar to the algorithms based on the Retinex theory. GWR, an algorithm combining both the Gray World assumption and the Retinex theory, produced a similar color difference as those based on the Gray World assumption.

Figure 5 shows the average color difference of the three whiteness standards, together with the difference of each standard, between the two balanced images using each algorithm. It can be observed that the three whiteness standards always had noticeable color differences under the two illuminants regardless of the algorithms and the difference of the three standards varied with the algorithms. It was interesting to find that $W_{138.9}$, the whiteness standard containing the greatest amount of FWAs, did not always have the largest color difference under the two illuminants. The greater the amount of FWAs, the larger the color difference with the algorithms based on the Gray World assumption. In contrast, greater amount of FWAs caused smaller color difference with the algorithms based on the Retinex theory. For the SoG algorithms, a higher p value reduced the color difference of $W_{138.9}$, but increased that of $W_{84.4}$.

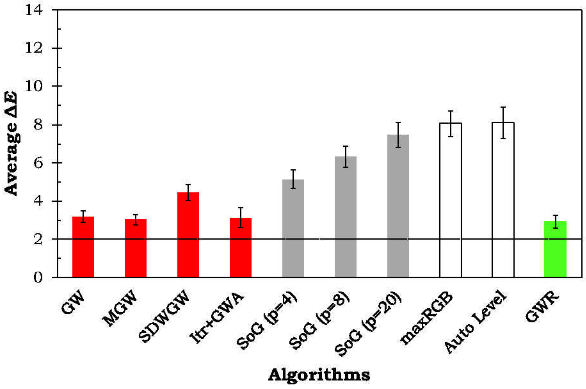

Figure 4 The average color difference of the 24 Macbeth patches and the three whiteness standards, together with the error bars, between the two balanced images using each algorithm in CIELAB color space (Note: the algorithms based on the Gray World assumption are in red; those based on the Retinex theory are in white; the SoG and GWR algorithms are in gray and green respectively). The dotted line represents the just-noticeable color difference (i.e., ΔE ≈ 2) [18].

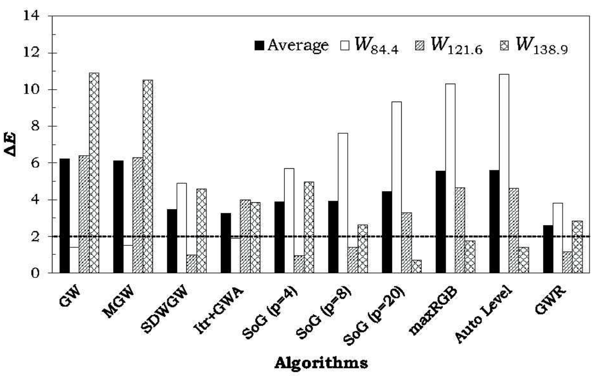

Figure 5 The color difference of the three whiteness standards between the two balanced images using each algorithm in CIELAB color space. The dotted line represents the just noticeable color difference (i.e., ΔE ≈ 2).

In addition to the color difference of a same whiteness standard between the two images, the color difference between the three whiteness standards in one image also matters, as they contained different amount of FWAs and should have different whiteness appearance. As summarized in Table II, all the algorithms, except the Itr+GWA, produced similar color differences between the three whiteness standards in each image. The three whiteness standards in the image captured under low UV/violet radiation had smaller color differences than those in the other image, which was due to the failure of low UV/violet level to excite FWAs.

Furthermore, the color differences between the three whiteness standards in the image captured under low UV/violet radiation was only caused by the lightness difference, while the color differences in the other image were caused by both lightness difference and chromaticity shift. As shown in Fig. 6, the chromaticities of the three whiteness standards in the image captured under low UV/violet radiation were close to each other, regardless of the white balance algorithms, while large chromaticity shifts can be observed in the other image. In can also be found that the chromaticity of $W_{84.4}$ was shifted towards the positive direction of b^* from the image under low UV/violet radiation to the other image when using the algorithms based on the Gray World assumption, but had little shifts when using the algorithms based on the Retinex theory.

Table II The color difference ΔE, together with the differences in L^*, a^*, and b^* between $W_{121.6}$ and $W_{84.4}$, and between $W_{138.9}$ and $W_{84.4}$ in the two balanced images when using each algorithm.

		W 121.6 - W 84.4				W 138.9 - W 84.4			
	Algorithms	ΔE	ΔL	Δa	Δb	ΔE	ΔL	Δa	Δb
Low UV/violet	GW	6.2	6.2	-0.6	0.3	10.6	10.5	-0.6	0.6
	MGW	6.4	6.2	-1.6	0.7	10.8	10.5	-2.1	1.2
	SDWGW	5.5	5.5	-0.5	0.2	9.4	9.4	-0.3	0.5
	Itr+GWA	1.5	1.0	-1.2	0.1	2.1	1.4	-1.5	-0.3
	SoG (p=4)	6.2	6.2	-0.7	0.3	10.6	10.5	-0.5	0.5
	SoG (p=8)	6.2	6.2	-0.6	0.3	10.6	10.5	-0.4	0.5
	SoG (p=20)	6.2	6.2	-0.6	0.3	10.6	10.6	-0.4	0.5
	maxRGB	6.2	6.2	-0.7	0.3	10.6	10.5	-0.6	0.6
	Auto Level	6.7	6.6	-0.6	0.2	11.3	11.3	-0.4	0.4
	GWR	6.2	6.2	-0.6	0.3	10.6	10.6	-0.4	0.6
		W 121.6 - W 84.4				W 138.9 - W 84.4			
	Algorithms	ΔE	ΔL	Δa	Δb	ΔE	ΔL	Δa	Δb
Normal UV/violet	GW	9.1	6.5	1.2	-6.3	15.2	10.9	3.3	-10.1
	MGW	8.7	6.6	0.3	-5.7	14.3	10.9	1.4	-9.1
	SDWGW	8.0	5.9	1.1	-5.2	13.3	9.9	2.8	-8.5
	Itr+GWA	5.2	0.4	2.0	-4.8	5.2	0.5	2.0	-4.8
	SoG (p=4)	9.0	6.6	1.2	-6.0	14.8	11.0	3.0	-9.5
	SoG (p=8)	8.9	6.6	1.1	-5.8	14.7	11.0	2.9	-9.2
	SoG (p=20)	8.8	6.6	1.0	-5.6	14.5	11.1	2.7	-9.0
	maxRGB	8.7	6.6	0.7	-5.5	14.3	11.1	2.2	-8.7
	Auto Level	9.4	7.2	1.0	-6.1	15.6	11.9	2.7	-9.6
	GWR	7.8	6.8	0.1	-3.9	12.7	11.4	0.8	-5.6

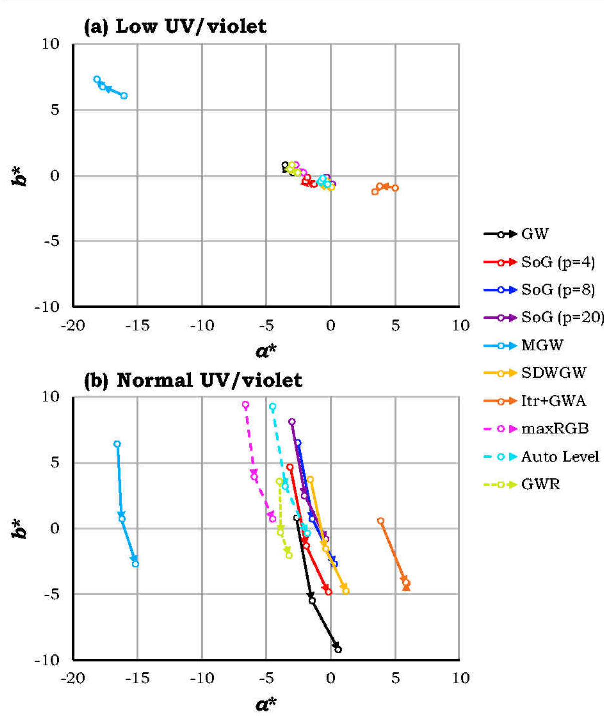

Figure 6 The chromaticity shifts from $W_{84.4}$ to $W_{121.6}$ and $W_{138.9}$ in the a-b* plane of CIELAB color space (a) In the image captured under low UV/violet radiation and (b) in the image captured under normal UV/violet radiation.*

Discussion

Since the setup in this study included colors with various hues and a neutral gray background, both the Gray World assumption and the Retinex theory should be applicable. The color differences caused by the illuminants, however, varied with the algorithm. Though both the GW and maxRGB algorithms, the two simplest algorithms based on the Gray World assumption and Retinex theory respectively, linearly adjusted the RGB values of each pixel using the gain factors (i.e., *corrR* and *corrB*), the gain factors were calculated in different ways and had large differences, as can be observed in Table III. When using the GW algorithm, the FWA excitation in the image captured under normal UV/violet radiation failed to change the average RGB values of the entire image as only 4.5% pixels of the image were covered by three whiteness standards. In contrast, the maxRGB algorithm calculated the gain factors based on the highest RGB values of the image, as shown in Fig. 7, and the FWA excitation in the image captured under normal UV/violet radiation increased the maximum B value, which resulted in a relatively large decrease in *corrB*.

Table III The average and maximum RGB values in the two images and the calculated gain factors by GW and maxRGB algorithms.

		Low UV/violet	Normal UV/violet	Difference
GW	Avg *R*	26	25	1
	Avg *G*	52	49	2
	Avg *B*	34	34	0
	corrR	1.98	1.97	0.01
	corrB	1.53	1.47	0.06
maxRGB	Max *R*	128	127	1
	Max *G*	255	255	0
	Max *B*	166	191	-25
	corrR	1.99	2.01	-0.02
	corrB	1.54	1.34	0.20

The color differences using the SoG algorithms were generally between those using the GW and the maxRGB algorithms, as shown in Fig. 8. The *corrR* had little differences between the two images regardless of the algorithms, while the *corrB* had much larger differences between the two images. The higher UV/violet radiation in the image captured under normal UV/violet radiation increased the *B* values of the three whiteness standards, which were given higher weights to calculate *corrB* with an increase in Minkowski norm *p*, as illustrated in Eq. (1).

The color differences of the three whiteness standards between the two images, as shown in Fig 5, are not trivial. Though the FWA excitation introduced a similar average color difference of the three standards with the GW and maxRGB algorithms, the differences of each individual standard were not similar. The GW algorithm balanced the images based on the average RGB values, so that color difference introduced by the FWA excitation was not further adjusted. On the contrary, the maxRGB algorithm balanced the images using the highest RGB values in the images, which happened to $W_{138.9}$, so that $W_{138.9}$ became neutral after white balancing.

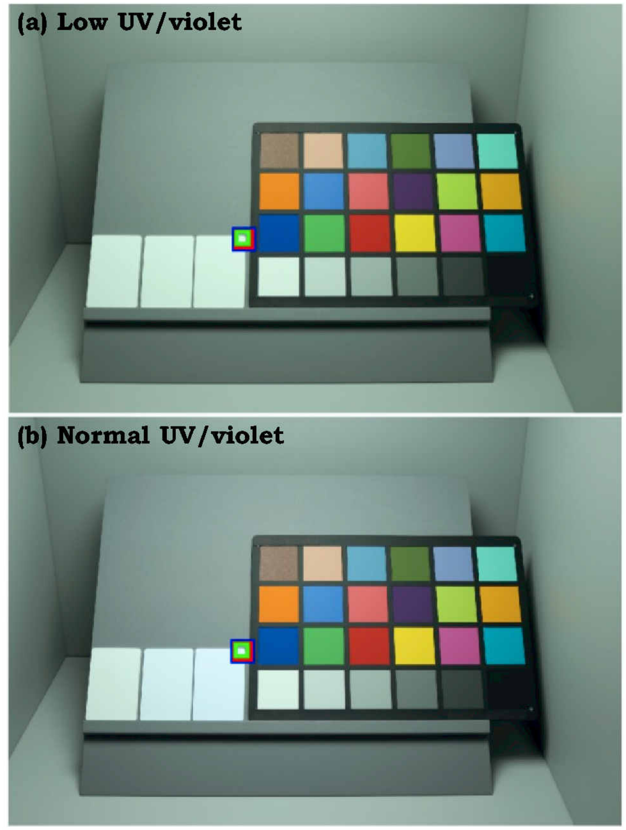

Figure 7 The positions of the pixels with the highest R, G, and B values (note: the pixels are located at the center of the highlighted area) (a) In the image captured under low UV/violet radiation; (b) in the image captured under normal UV/violet radiation.

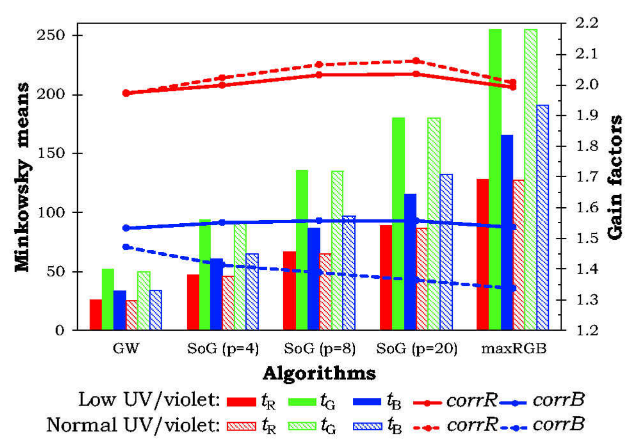

Figure 8 The calculated Minkowski means and gain factors when using the GW, SoG, and maxRGB algorithms in the two images.

The FWA excitation also affected the color difference between the three whiteness standards in each image, as shown in Table II and Fig 6. The three whiteness standards in the image captured under low UV/violet radiation only had little differences in lightness with different algorithms, which revealed the problem of a typical white-light LED to render whiteness for an imaging system. The noticeable lightness and chromaticity differences among the three whiteness standards with different amount of FWAs in the image taken under the illuminant with a normal level of UV/violet radiation, can differentiate the color differences and degrees of whites perceived by human beings.

Conclusion

Various white balance algorithms were applied to two images that captured a same setup under two 6500 K illuminants with one illuminant simulating the amount of UV/violet radiation contained in CIE standard D65 and the other simulating the typical commercially available white-light LEDs.

It was found that the lower level of UV/violet radiation contained in the illuminant produced noticeable color differences to various colors, especially when the algorithms based on the Retinex theory was applied. Specifically, the three whiteness standards containing different amount of FWAs had much smaller chromaticity differences and color differences under the illuminant with lower UV/violet radiation. The chromaticities of these whites were shifted towards the positive direction of b^*, with the standards containing more FWAs having greater shifts under the algorithms based on the Gray World assumption and smaller shifts under those based on the Retinex theory.

The color differences shown in this study clearly revealed that the failure of typical white-light LEDs to excite FWAs caused noticeable color differences to imaging systems regardless of the white balance algorithms, which may affect the overall image quality.

Funding

Research Grant Council of the Hong Kong Special Administrative Region, China (PolyU 252029/16E).

References

[1] M. Wei, KW. Houser, A. David, and MR. Krames, “Blue-pumped white LEDs fail to render whiteness,” in Proceedings of CIE 2014 Lighting and Energy Efficiency, Kuala Lumpur, Malaysia, pp. 150-159, 2014.

[2] M. Wei, KW. Houser, A. David, and MR. Krames, "Whiteness perception under LED illumination," Leukos, vol. 10, no.3, pp. 165-180, 2014.

[3] M. Wei, KW. Houser, A. David, and MR Krames, "Perceptual responses to LED illumination with colour rendering indices of 85 and 97," Lighting Res Technol, vol. 47, no.7, pp. 810-827, 2014.

[4] M. Wei and Y. Wang, "Judgement of white appearance for surface colors under individual and simultaneous observations," Leukos, doi: 10.1080/15502724.2018.1455514, 2018.

[5] HP. Huang, M. Wei, and LC. Ou, "White appearance of a tablet display under different ambient lighting conditions," Opt. Express, vol. 26, no.4, pp. 5018-5030, 2018.

[6] G. Buchsbaum, “A spatial processor model for object colour perception,” J. Franklin Inst., vol. 310, no. 1, pp. 1–26, 1980.

[7] EH. Land and JJ. McCann, “Lightness and Retinex theory,” JOSA, vol. 61, no.1, pp. 1–11, 1971.

[8] G. Zapryanov, D. Ivanova, and I. Nikolova, “Automatic white balance algorithms for digital still cameras - a comparative study,” Inf. Techno. Control, vol. 1, pp. 16-22, 2012.

[9] R. Lukac, Single-Sensor Imaging: Methods and Applications for Digital Cameras, CRC Press, 2008.

[10] HK. Lam, OS. Au, and CW. Wong, "Automatic white balancing using standard deviation of RGB components," IEEE Int. Symp. Circ. S., vol. 3, pp. 921-924, 2004.

[11] GD. Finlayson and E. Trezzi, “Shades of Gray and Colour Constancy,” in 12th Color and Imaging Conference, Scottsdale (AZ), USA, pp. 37-41, 2004.

[12] J. Lee, Y. Jung, B. Kim, and H. Zen, “An advanced video camera system with robust AF, AE, and AWB control,” IEEE Consum. Electr., vol. 47, no. 3, pp. 694-699, 2001.

[13] J. Huo, Y. Chang, J. Wang, and F. Yu, “Robust automatic white balance algorithm using gray color points in images,” IEEE Consum. Electr., vol. 52, no. 2, pp. 541-546, 2006.

[14] N. Limare, J. Lisani, J. Morel, A. Petro, and C. Sbert, “Simplest color balance,” Image Processing On Line, vol. 1, pp. 297-315, 2011.

[15] EY. Lam, “Combining gray world and Retinex theory for automatic white balance in digital photography,” in Proceedings of the 9th International Symposium on Consumer Electronics, Macau, China, pp. 134-139, 2005.

[16] M. Wei, S. Ma, Y. Wang, and MR. Luo, “Evaluation of whiteness formulas for FWA and non-FWA whites,” JOSA A, vol. 34, no.4, pp. 640-647, 2017.

[17] M. Wei and KW. Houser, “Status of solid-state lighting based on entries to the 2010 US DOE Next Generation Luminaire Competition,” Leukos, vol. 8, no.4, pp. 237-259, 2012.

[18] G. Sharma and R. Bala, Digital color imaging handbook, CRC Press, 2003.

Author Biography

Siyuan Chen is currently a PhD candidate in Department of Building Services Engineering at the Hong Kong Polytechnic University. He obtained his Bachelor of Engineering at Tongji University (Shanghai, China) in 2016.

Minchen Wei is an Assistant Professor in Department of Building Services Engineering at the Hong Kong Polytechnic University. He earned his Bachelor of Engineering at Fudan University (Shanghai, China) in 2009. In 2011 and 2015, he obtained his Master of Science and Doctoral Degrees from Department of Architectural Engineering at the Pennsylvania State University (University Park, USA). His research mainly focuses on color science and illumination.